CHAPTER 6

DEWATERING AND COMPACTION OF SEDIMENT

(With major contributions by Johannes Wendebourg)

In this chapter we deal with those post-depositional processes that involve compaction of sediment and expulsion of porewater, both of which are closely linked. Clearly, processes that affect sedimentation do not stop with deposition of sediment. Newly deposited sediment occupies space within a basin, but this space is progressively reduced as compaction takes place in response to the load of overlying sediment. Of course, some of the water in pore spaces in the sediment must be displaced if compaction is to occur, so that dewatering and compaction are aspects of the same basic process.

Because space must be available in a basin if sediment is to be deposited, any space occupied by previous deposits affects opportunities for new deposits to form. If compaction of previous deposits has occurred, more space may be locally available than if compaction has not occurred. Thus, depositional processes are strongly, although indirectly, affected by dewatering and compaction. Therefore, dewatering and compaction are important components of integrated dynamic models of sedimentary basins, even if not of primary interest in themselves. While the relatively simple model and computer program that combine compaction and dewatering that are presented here are not linked directly with other models and computer programs of depositional processes, enterprising users could provide such linkages.

In this chapter, we treat flow through porous materials and the concept of fluid potential. While we are principally concerned with flow in porous materials driven by compaction, we shall also treat flow driven by differences in hydraulic head that stem from differences in topography. Because our broad concern is with the role of flow of porewater in sedimentary basins, we shall begin by discussing the basics of flow in porous materials.

In addition to treating compaction and fluid flow, we also discuss the thermal regime within sedimentary basins. The thermal evolution of sedimentary basins is

often recorded by thermally sensitive indicators that are both organic and inorganic. By linking the thermal and physical evolution of basins, we can use these thermal indicators to interpret the development of the basin. Also, thermal processes affect the presence of oil and gas and can provide insight into the maturation level of hydrocarbon sources.

DARCY'S LAW

In 1856, Henry Darcy established an empirical relationship between the flow of water through a column of sand or other porous material, and the difference in hydraulic head between the top and bottom end of the column (Figure 6-1). "Hydraulic head" may be defined as the elevation to which water would rise as a result of pressure and gravitational forces acting on it (Hubbert, 1940). Equation (6-1) expresses this relationship, which is familiarly known as Darcy's law:

$$Q = \frac{KA\Delta h}{L} \tag{6-1}$$

where: Q = volume of water flowing through column in m^3/s,
A = cross-sectional area of column in m^2,
L = length of column in m,
Δh = difference in hydraulic head between top and bottom of column in m,
K = proportionality factor that depends on properties of both porous material and fluid in column in m/s.

The filtration velocity of flow u through the column is obtained by dividing Q by the cross-sectional area:

$$u = \frac{Q}{A} \tag{6-2}$$

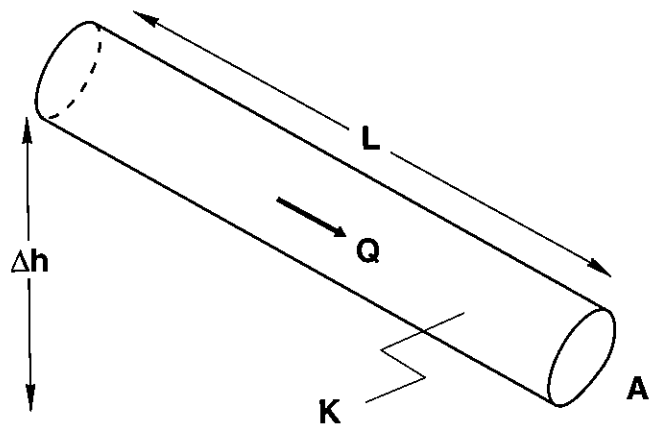

Figure 6-1 Diagram illustrating Darcy's experiment in which water flows through tube of length L and cross-sectional area A, and is filled with porous material of property K, through which volume Q flows in response to difference in hydraulic head h

The fluid itself, however, moves only in the pore spaces within the material, so that the true fluid velocity v is obtained by dividing the filtration velocity by the porosity ϕ:

$$v = \frac{u}{\phi} \tag{6-3}$$

Fluids that move through porous materials obey the same laws as fluids flowing in the open. This property permits us to recast Darcy's law in form of the Bernoulli equation (see Chapter 4). The Bernoulli equation balances all forces acting on a fluid volume and is expressed in the form of a total hydraulic head that is the sum of a pressure head, a velocity head, and an elevation head. Because groundwater velocities are usually very small, we can neglect the velocity head, writing the Bernoulli equation as:

$$h = \frac{p}{\rho_w g} + \frac{v^2}{2g} + z \cong \frac{p}{\rho_w g} + z \tag{6-4}$$

where: h = total hydraulic head in m,
p = pressure in Pa (pascals),
g = acceleration of gravity in m/s^2,
ρ_w = water density in kg/m^3,
z = elevation in m.

This permits us to write Darcy's law in a more generalized form:

$$u = -\frac{k}{\mu}(\nabla p - \rho_w g \nabla z) \tag{6-5}$$

where: k = intrinsic permeability that is a property of the porous medium in m^2,
μ = dynamic viscosity in cP (centipoises) or Pa's.

Note the negative sign because flow occurs in the direction of decreasing fluid potential.

LINKING FLUID FLOW WITH COMPACTION

Our next task is to link fluid flow in porous materials with compaction. We begin by considering Terzaghi's concept of consolidation in soils (Terzaghi and Peck, 1967), where compaction stems from compression of the soil and pore volume is reduced in proportion to the increase in effective stress:

$$-\frac{dV_p}{V} = \alpha d\sigma_e \tag{6-6}$$

where: σ_e = effective stress in Pa,
α = soil compressibility in Pa^{-1},
V = bulk volume in m^3,
V_p = pore volume in m^3.

We assume that compaction acts only vertically and that lateral effects can be neglected because they are small compared with effects that stem from rearrange-

ment of grains by vertical loading. Compaction of water-saturated soil or other porous materials, however, only partially stems from the overlying sediment load, because some part of the stress is carried by the pore fluid. Since total stress is the sum of effective stress and pore-fluid pressure, and since total stress remains constant during compaction, any change in effective stress must be compensated by an equal change in pore-fluid pressure:

$$\sigma = \sigma_e + p = \text{constant} \tag{6-7}$$

or

$$d\sigma_e = -dp \tag{6-8}$$

where: p = fluid pressure in Pa,
σ = total stress in Pa.

Pore pressure dissipates slowly as the pore water escapes upward. Only when fluid pressure reaches hydrostatic conditions is the material fully compacted under the applied load.

POROSITY AND COMPACTION

Now it is appropriate to explore the relationships between porosity and compaction. We can define porosity, ϕ, as the proportion of the volume of a water-saturated sediment occupied by the pore water:

$$\phi = \frac{V_p}{V} \tag{6-9}$$

where: V = bulk volume in m^3,
V_p = pore volume in m^3.

Change in porosity can be calculated by differentiating with respect to pore volume (deMarsily, 1986):

$$\frac{d\phi}{dV_p} = \frac{d}{dV_p}\left(\frac{V_p}{V}\right) = \frac{V - V_p}{V^2} = \frac{V(1-\phi)}{V^2} = \frac{1-\phi}{V} \tag{6-10}$$

Using the definitions of compaction and effective stress in (6-6) to (6-10), we can write the change in porosity as a function of change in pore-fluid pressure:

$$d\phi = -(1-\phi)\,\alpha d\sigma_e = (1-\phi)\,dp \tag{6-11}$$

If we assume that the change in porosity yields a rate of subsidence that is small compared to the fluid velocity, we can take the partial derivative (Freeze and Cherry, 1979), yielding the equation of state for the porous medium:

$$\frac{\partial \phi}{\partial t} = (1-\phi)\,\alpha \frac{\partial p}{\partial t} \tag{6-12}$$

Equation (6-12) can be combined with two other equations to yield the governing flow equation in a compacting medium. The first is the continuity equation for the fluid:

$$\nabla(\rho_w \dot{u}_w) + \frac{\partial}{\partial t}(\rho_w \phi) = 0 \tag{6-13}$$

In (6-13) we can insert the momentum equation for the fluid (6-5), which is Darcy's law. The second is an equation of state for the pore water. Here, we assume an incompressible fluid.

$$\rho_w = \text{constant} \tag{6-14}$$

Now, (6-12) through (6-14) yield the classical consolidation equation:

$$\nabla\left[\frac{k}{\mu}\nabla p\right] = (1-\phi)\,\alpha\frac{\partial p}{\partial t} \tag{6-15}$$

Equation (6-15) is used in groundwater hydraulics to describe the effects of aquifer compaction due to withdrawal of groundwater, which reduces fluid pressure, thereby increasing effective stress and, in turn, possibly leading to accelerated ground subsidence. An example of accelerated subsidence due to excessive pumping in Venice has been described by Gambolati and Freeze (1973).

COUPLED MOVEMENT OF SOLID MATERIAL AND PORE WATER IN BASINS

Equation (6-15) assumes that solid material moves at much slower rates than the fluid. However, in sedimentary basins that evolve through geologic time, solid material may move at rates comparable to, or even faster than, those of pore fluids. This requires that we solve the combined continuity equations for both pore fluids and solid material (Bear, 1972; deMarsily, 1986). The fluid continuity equation is (6-13), and the solid continuity equation is:

$$\nabla(\rho_s \dot{\vec{u}}_s) + \frac{\partial}{\partial t}[\rho_s(1-\phi)] = 0 \tag{6-16}$$

where: ρ_s = sediment density in kg/m^3,
ϕ = porosity,
u_s = velocity of solid material in m/s.

Again using the momentum equation for the pore fluid (6-5), coupled with the fact that the true fluid velocity is u_w/ϕ, then the fluid motion can be expressed relative to the moving solid material:

$$\dot{\vec{u}}_w = \phi(\dot{\vec{v}}_w - \dot{\vec{v}}_s) = -\frac{k}{\mu}(\nabla p - \rho_w g \nabla z) \tag{6-17}$$

where: v_w = true fluid velocity in m/s,
v_s = true solid velocity in m/s.

We can insert the momentum equation into the fluid-continuity equation and expand the solid-velocity term:

$$\rho_w\phi\nabla\,\dot{\vec{v}}_s + \dot{\vec{v}}_s\nabla\,(\rho_w\phi) - \nabla\left[\rho_w\frac{k}{\mu}(\nabla p - \rho_w g\nabla z)\right] + \frac{\partial}{\partial t}(\rho_w\phi) = 0 \tag{6-18}$$

So far, we have considered a fixed coordinate system through which both fluid and solid are moving. If we want to express (6-18) in terms of the moving fluid only, we have to consider a volume of porous material that is moving

through the coordinate system. This allows us to take the total derivative with respect to the solid material (deMarsily, 1986):

$$\frac{d}{dt}(\rho_w \phi) = \frac{\partial}{\partial t}(\rho_w \phi) + \dot{v}_s \nabla (\rho_w \phi) \tag{6-19}$$

By expanding the expression, we get:

$$\frac{d}{dt}(\rho_w \phi) = \rho_w \frac{d\phi}{dt} + \phi \frac{d\rho_w}{dt} \tag{6-20}$$

Using an equation of state for the pore fluid, where fluid density is defined by an exponential law (Freeze and Cherry, 1979), we obtain:

$$\rho_w = \rho_0 exp\,[\beta (p - p_0)] \tag{6-21}$$

where: p_0 = reference pressure in Pa,
β = fluid compressibility in Pa^{-1}.

Because density is now a function of fluid pressure, we can express its derivative also as a function of fluid pressure:

$$\phi \frac{d\rho_w}{dt} = \phi \rho_w \beta \frac{dp}{dt} \tag{6-22}$$

An equation of state for the solid material is more difficult to derive. Let us start with the continuity equation for the solid material (6-16) and expand it:

$$\rho_s (1-\phi) \nabla \dot{v}_s + \dot{v}_s \nabla [\rho_s (1-\phi)] + \frac{\partial}{\partial t}[\rho_s (1-\phi)] = 0 \tag{6-23}$$

Analogous to the fluid equation (6-19), we can replace the partial derivatives by the total derivative:

$$\frac{d}{dt}[\rho_s (1-\phi)] = \frac{\partial}{\partial t}[\rho_s (1-\phi)] + \dot{v}_s \nabla [\rho_s (1-\phi)] \tag{6-24}$$

We assume an equation of state for the solid material where the solid material is incompressible, which in turn presumes that the grains do not deform under the overlying load:

$$\rho_s = \text{constant} \tag{6-25}$$

We can then simplify the continuity equation for the solid material:

$$\rho_w \phi \nabla \dot{v}_s = \frac{\rho_w \phi}{(1-\phi)} \frac{d\phi}{dt} \tag{6-26}$$

Now we can replace this expression in (6-18) and simplify its compaction term:

$$\rho_w \frac{d\phi}{dt} + \frac{\rho_w \phi}{(1-\phi)} \frac{d\phi}{dt} = \frac{\rho_w}{(1-\phi)} \frac{d\phi}{dt} \tag{6-27}$$

Using Terzaghi's principle of consolidation from (6-7), we obtain:

$$\sigma_e = \sigma - p \tag{6-28}$$

Using (6-28), we can expand the derivative of porosity with respect to time:

$$\frac{d\phi}{dt} = \frac{d\phi}{d\sigma_e}\frac{d\sigma_e}{dt} = \frac{d\phi}{d\sigma_e}\frac{d(S-p)}{dt} \tag{6-29}$$

If we assume that porosity follows an exponential law as a function of effective stress (Schneider et al., 1991):

$$\phi = \phi_0 exp\,[-(\sigma_e/\sigma_e^0)] \tag{6-30}$$

where σ_e^0 = effective stress at reference porosity,

then we can determine its derivative with respect to effective pressure explicitly:

$$\frac{d\phi}{d\sigma_e} = -\frac{\phi}{\sigma_e^0} \tag{6-31}$$

Finally, the total load $\sigma = S$ is given by the integral over all overlying sediment layers, which is a known quantity:

$$S = \int_z \rho_s (1-\phi)\, g\, dz \tag{6-32}$$

Now we can write the general diffusion equation for pore-fluid motions in an evolving sedimentary basin:

$$\frac{1}{\rho_w}\nabla\left[\rho_w \frac{k}{\mu}(\nabla p - \rho_w g \nabla z)\right] - \left[\phi\beta - \frac{1}{1-\phi}\frac{d\phi}{d\sigma_e}\right]\frac{dp}{dt} = \frac{1}{1-\phi}\frac{d\phi}{d\sigma_e}\frac{dS}{dt} \tag{6-33}$$

Equation (6-33) does not explicitly consider topographically driven flow for which the hydraulic head is needed, which is the sum of the pressure head and the elevation head. Topographically driven flow can be introduced by setting the boundary conditions such that the pressures at the topographic boundary reflect the elevation head (Bethke, 1989). However, flow induced by elevation head generally is small relative to pressure-induced gradients within the ranges of depths and permeabilities of evolving sedimentary basins. However, as sedimentary basins approach maturity, earlier overpressures may have dissipated as sedimentation rates decrease, and may be replaced by steady-state flow fields that are driven by differences in topographic elevation. These steady-state flow fields may persist to substantial depths (Toth, 1978).

IMPLEMENTATION OF SIMPLIFIED DIFFUSION EQUATION

The general diffusion equation for an evolving sedimentary basin (6-33) has been implemented in a computer program in a simplified form. The equation is solved for a vertical cross section through a basin. In addition, the fluid is assumed to be incompressible, so that fluid potential can be represented by the pressure potential only. Applying these simplifications and expanding (6-33), we obtain:

$$\frac{\partial}{\partial x}\left[\frac{k_x}{\mu}\frac{\partial p}{\partial x}\right] + \frac{\partial}{\partial z}\left[\frac{k_z}{\mu}\frac{\partial p}{\partial z}\right] + \frac{1}{1-\phi}\frac{d\phi}{d\sigma_e}\frac{dp}{dt} = \frac{1}{1-\phi}\frac{d\phi}{d\sigma_e}\frac{dS}{dt} \tag{6-34}$$

which is the governing equation for pore-fluid motion where compaction is coupled with fluid flow in a two-dimensional vertical section across an evolving sedimentary basin. Note that we assume uniform thermal conditions so that viscosity of the pore fluid remains constant.

Permeability is assumed to be a function of porosity, which is usually derived from log-linear cross plots of permeability versus porosity (Bethke, 1985), according with the general equation:

$$\log k = a + b\phi \tag{6-35}$$

Since we assume that the porous material is anisotropic, permeability can be represented as a two-dimensional tensor if the grid representing the vertical section is oriented along the principal axes of flow:

$$[k] = \begin{bmatrix} f_h & 0 \\ 0 & f_v \end{bmatrix} k(\phi) \tag{6-36}$$

where: f_h = anisotropy coefficient for horizontal direction (usually 1),
f_v = anisotropy coefficient for vertical direction (usually < 1).

Equation (6-34) can be solved only with appropriate initial and boundary conditions. At the lower boundary (represented by an impermeable basement), there is no flow:

$$q_z = 0 \tag{6-37}$$

where q_z = volume flux in the vertical direction in m^3/s.

At the upper boundary (represented by the top of the sequence of sedimentary deposits), the pressure is assumed to be hydrostatic:

$$p = \rho_w g z \tag{6-38}$$

At the lateral boundaries, the pressure gradient is assumed to be constant:

$$\nabla p = \text{constant} \tag{6-39}$$

OBTAINING NUMERICAL SOLUTIONS OF THE DIFFUSION EQUATION

Program 24, Compaction and Fluid Flow Program, which is included in the Programs diskette accompanying this book, solves (6-34) in a discrete form employing finite differences. Finite-difference approximations can be derived directly from the differential equation, but can be used only when the grid is orthogonal. Alternatively, a local mass-balance procedure may be used if the grid is not orthogonal, which is the situation here. While we represent the sedimentary basin in a two-dimensional section that has equally spaced columns along the x axis (horizontal dimension), the z axis (vertical dimension) is represented by beds whose thicknesses vary both laterally as well as from layer to layer. The grid is therefore nonorthogonal, which permits both the basement topography and the aggregate thickness of basin fill to vary along the section. The local mass-balance procedure therefore is used for each individual layer.

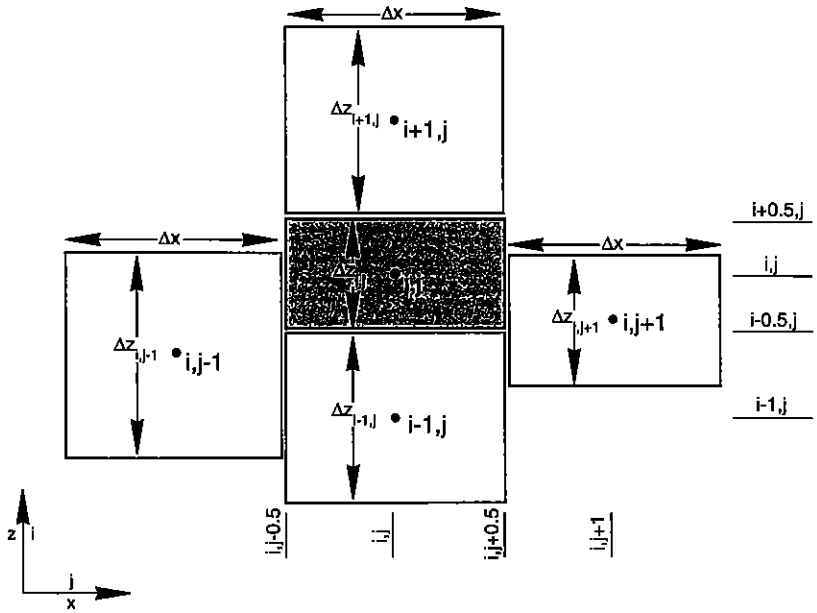

Figure 6-2 Definition of grid cell geometry and indices. Grid cell i,j and its four neighbor cells are shown. Note that horizontal grid spacing is constant, whereas vertical grid spacing depends on thickness of cell and therefore is variable.

The flow terms of the left-hand side of (6-34) can be expanded by performing a mass-balance for a single grid cell. Properties for such a cell are defined at its center, whereas the fluxes through the cell are defined at its boundaries. The horizontal or x direction has index j, and the vertical or z direction has index i (Figure 6-2). In the horizontal direction, inflow is from the right boundary of a cell ($q_{i,j+0.5}$) and outflow is at the left boundary ($q_{i,j-0.5}$):

$$\frac{d}{dx}\left[\frac{k_z}{\mu}\frac{\partial p}{\partial x}\right] \cong q_{i,j+0.5} - q_{i,j-0.5} \tag{6-40}$$

where: k_x = intrinsic permeability in x direction in m^2,

q = volume flux in m^3/s.

Inflow is given by:

$$q_{i,j+0.5} = \Delta z_{i,j+0.5}\frac{k_{xi,j+1}\Delta x}{\mu}\left[\frac{p_{i,j+1}-p_{i,j+0.5}}{\Delta x/2}\right] - \Delta z_{i,j+0.5}\left(\frac{k_{xi,j}\Delta x}{\mu}\left[\frac{p_{i,j+0.5}-p_{i,j}}{\Delta x/2}\right]\right) \tag{6-41}$$

$$q_{i,j+0.5} = 2\left[\left(\frac{1}{k_{i,j}\Delta z_{i,j+0.5}}\right) + \left(\frac{1}{k_{i,j+1}\Delta z_{i,j+0.5}}\right)\right]^{-1}\mu^{-1}(p_{i,j+1}-p_{i,j}) \tag{6-42}$$

with:

$$\Delta z_{i,j+0.5} = (\Delta z_{i,j} + \Delta z_{i,j+1})/2 \tag{6-43}$$

and outflow is given by:

$$q_{i,j-0.5} = \Delta z_{i,j-0.5}\frac{k_{xi,j}\Delta x}{\mu}\left[\frac{p_{i,j}-p_{i,j-0.5}}{\Delta x/2}\right] - \Delta z_{i,j-0.5}\frac{k_{xi,j-1}\Delta x}{\mu}\left[\frac{p_{i,j-0.5}-p_{i,j-1}}{\Delta x/2}\right] \quad (6\text{-}44)$$

$$q_{i,j-0.5} = 2\left[\left(\frac{1}{k_{i,j}\Delta z_{i,j-0.5}}\right) + \left(\frac{1}{k_{i,j-1}\Delta z_{i,j-0.5}}\right)\right]^{-1}\mu^{-1}(p_{i,j}-p_{i,j-1}) \quad (6\text{-}45)$$

with:

$$\Delta z_{i,j-0.5} = \Delta (z_{i,j}+\Delta z_{i,j-1})/2 \quad (6\text{-}46)$$

Similarly, in the vertical direction, inflow is from the upper boundary of a volume element ($q_{i+0.5,j}$) and outflow is at the lower boundary ($q_{i-0.5,j}$):

$$\frac{\partial}{\partial z}\left[\frac{k_z}{\mu}\frac{\partial p}{\partial z}\right] \cong q_{i+0.5,j} - q_{i-0.5,j} \quad (6\text{-}47)$$

where inflow is given by:

$$q_{i+0.5,j} = \Delta x\frac{k_{zi+1,j}\Delta x}{\mu}\left[\frac{p_{i+1,j}-p_{i+0.5,j}}{\Delta z_{i+1,j}/2}\right] - \Delta x\frac{k_{zi,j}\Delta x}{\mu}\left[\frac{p_{i+0.5,j}-p_{i,j}}{\Delta z_{i,j}/2}\right] \quad (6\text{-}48)$$

$$q_{i+0.5,j} = \frac{2(\Delta x)^2}{\left(\frac{\Delta z}{k}\right)_{i+1,j} + \left(\frac{\Delta z}{k}\right)_{i,j}}\mu^{-1}(p_{i+1,j}-p_{i,j}) \quad (6\text{-}49)$$

and outflow is given by:

$$q_{i-0.5,j} = \Delta x\frac{k_{zi,j}\Delta x}{\mu}\left[\frac{p_{i,j}-p_{i-0.5,j}}{\Delta z_{i,j}/2}\right] - \Delta x\frac{k_{zi-1,j}\Delta x}{\mu}\left[\frac{p_{i-0.5,j}-p_{i-1,j}}{\Delta z_{i-1,j}/2}\right] \quad (6\text{-}50)$$

$$q_{i-0.5,j} = \frac{2(\Delta x)^2}{\left(\frac{\Delta z}{k}\right)_{i,j} + \left(\frac{\Delta z}{k}\right)_{i-1,j}}\mu^{-1}(p_{i,j}-p_{i-1,j}) \quad (6\text{-}51)$$

Accumulation due to compaction is approximated by:

$$\frac{1}{1-\phi}\left(\frac{d\phi}{d\sigma_e}\right)\frac{dS}{dt} \cong \frac{V_{pi,j}}{1-\phi_{i,j}}\left(\frac{-\phi_{i,j}}{\sigma_e^0}\right)\frac{p_{i,j}^{n+1}-p_{i,j}^{n}}{\Delta t} \quad (6\text{-}52)$$

The sediment-load term is approximated by:

$$\frac{1}{1-\phi}\left(\frac{d\phi}{d\sigma_e}\right)\frac{dS}{dt} \cong \frac{V_{pi,j}}{1-\phi_{i,j}}\left(\frac{-\phi_{i,j}}{\sigma_e^0}\right)\frac{\rho_s g \Delta z_{k,j}(1-\phi_{k,j})}{\Delta t} \tag{6-53}$$

where: k = index of layer that loads sediment column,
S = sediment load in Pa,
z = thickness in m.

Pore volume is given by:

$$V_{pi,j} = \phi_{i,j} \Delta z_{i,j} (\Delta x)^2 \tag{6-54}$$

Boundary conditions are approximated as follows. At the lower boundary, there is no flow, and therefore:

$$q_{0.5,j} = 0 \tag{6-55}$$

At the upper boundary, fluid pressure is hydrostatic:

$$p_{k,j} = \rho_w g z_{0,j} \tag{6-56}$$

where: k = index of loading sediment layer,
$z_{0,j}$ = elevation at topography.

At the left boundary, the pressure is given by a constant gradient:

$$p_{i,0} = 2p_{i,1} - p_{i,2} \tag{6-57}$$

At the right boundary, the pressure is also given by a constant gradient:

$$p_{i,n+1} = 2p_{i,n} - p_{i,n-1} \tag{6-58}$$

where: n = number of columns in grid.

SOLVING THE SYSTEM OF EQUATIONS OVER THE GRID

For each grid node, there is one equation with five unknown pressures. Thus, we can establish a linear system of equations with as many equations as there are unknown pressures in the grid. Each equation is of the following form:

$$A_{i,j}p_{i,j-1} + B_{i,j}p_{i-1,j} + C_{i,j}p_{i,j} + D_{i,j}p_{i+1,j} + E_{i,j}p_{i,j+1} = F_{i,j} \tag{6-59}$$

with coefficients $A_{i,j}$ to $F_{i,j}$ defined as:

$$A_{i,j} = 2\left[\left(\frac{1}{k_{i,j}\Delta z_{i,j-0.5}}\right) + \left(\frac{1}{k_{i,j-1}\Delta z_{i,j-0.5}}\right)\right]^{-1}\mu^{-1} \tag{6-60}$$

$$B_{i,j} = \frac{2(\Delta x)^2}{\left(\frac{\Delta z}{k}\right)_{i-1,j} + \left(\frac{\Delta z}{k}\right)_{i,j}} \mu^{-1} \tag{6-61}$$

$$C_{i,j} = -(A+B+D+E) + \frac{V_{pi,j}}{1-\phi_{i,j}} \left(\frac{-\phi_{i,j}}{\sigma_e^0}\right) \Delta t^{-1} \tag{6-62}$$

$$D_{i,j} = \frac{2(\Delta x)^2}{\left(\frac{\Delta z}{k}\right)_{i+1,j} + \left(\frac{\Delta z}{k}\right)_{i,j}} \mu^{-1} \tag{6-63}$$

$$E_{i,j} = 2\left[\left(\frac{1}{k_{i,j}\Delta z_{i,j+0.5}}\right) + \left(\frac{1}{k_{i,j+1}\Delta z_{i,j+0.5}}\right)\right]^{-1} \mu^{-1} \tag{6-64}$$

$$F_{i,j} = \frac{V_{pi,j}}{1-\phi_{i,j}} \left(\frac{-\phi_{i,j}}{\sigma_e^0}\right) \Delta t^{-1} \left[\rho_s g \Delta z_{k,j} (1-\phi_{k,j}) + p_{i,j}^n\right] \tag{6-65}$$

The resulting system of equations yields a banded matrix that is pentadiagonal, with a bandwidth $m = 2n + 1$, where n = number of sediment layers:

$$\begin{bmatrix} \cdots & & & & & & \\ \cdots 0 \cdots & B & C & D & \cdots 0 \cdots & E & \\ A_{i,j} & \cdots 0 \cdots & B_{i,j} & C_{i,j} & D_{i,j} & \cdots 0 \cdots & E_{i,j} \\ & A & \cdots 0 \cdots & B & C & D & \cdots 0 \cdots \\ & & & & & & \end{bmatrix} \begin{bmatrix} \cdots \\ p_{i-1,j} \\ p_{i,j} \\ p_{i+1,j} \\ \cdots \end{bmatrix} = \begin{bmatrix} \cdots \\ \cdots \\ F_{i,j} \\ \cdots \\ \cdots \end{bmatrix} \tag{6-66}$$

In Program 24, Compaction and Fluid Flow Program, this system is solved directly by Gaussian elimination using LU deccomposition.

PETROPHYSICAL DATA REQUIRED FOR NUMERICAL EXPERIMENTS

To solve the system of equations represented by (6-66), porosity and permeability values are necessary properties of each grid cell. Table 6-1 contains data for porosity and effective stress, and Table 6-2 contains data for permeability. Data from both tables are provided internally in the program.

Table 6-1 Coefficients for exponential porosity-effective stress function adapted from Schneider and others (1991), that are supplied internally to Program 24, Compaction and Fluid Flow Program.

	Reference Porosity	Reference Effective Stress in MPa
North Sea sands (Brent)	0.43	27
North Sea shales (Jurassic)	0.58	18
Mahakam Delta sands	0.50	37
Mahakam Delta shales	0.45	26

Porosity is calculated as a function of effective vertical stress, which is the difference between the lithostatic pressure (total stress) of a specific grid cell and its fluid pressure:

$$\phi_{i,j} = \phi_k^0 exp\left[\frac{(p_{lith} - p)_{i,j}}{\sigma_{ek}^0}\right] \quad \textbf{(6-67)}$$

whereas permeability is calculated as a log-linear function of porosity:

$$k_{i,j} = f_k 10^{(a_k b_k \phi_{i,j})} \quad \textbf{(6-68)}$$

where: k = lithology indicator for sand or shale.

After the fluid pressure potential has been solved over the grid, flow velocities can be calculated for each grid cell. Pressures are determined at cell boundaries to get the x- and z-velocity components in the center of each cell:

$$v_{xi,j} = \frac{k_{xi,j}}{\phi_{i,j}\mu}\left[\frac{p_{i,j+0.5} - p_{i,j-0.5}}{\Delta x}\right] \quad \textbf{(6-69)}$$

$$v_{zi,j} = \frac{k_{zi,j}}{\phi_{i,j}\mu}\left[\frac{p_{i+0.5,j} - p_{i-0.5,j}}{\Delta z_{i,j}}\right] \quad \textbf{(6-70)}$$

Table 6-2 Coefficients for log-linear porosity-permeability function adapted from Bethke (1985) that are supplied internally to Program 24, Compaction and Fluid Flow Program.

	Anisotropy factor f_V	a	b
Sand	0.4	-13	2
Shale	0.1	-19	8

Table 6-3 Example input for Program 24, Compaction and Fluid Flow Program.

1st line:	
Number of columns in cross section	<10>
Number of layers that are deposited	<5>
Spacing of columns in m	<10000>
2nd line:	
Density of water in kg/m3	<1027>
Density of solid sediment in kg/m3	<2650>
Viscosity of water in cP	<1.0>
3rd line:	
Initial basement topographic elevation for each column in m (datum is sea level)	
Second part of input consists of four lines for each sediment layer that are to be deposited in same sequence, and are read in as follows:	
1st line:	
Time interval represented by sediment layer in millions of years	<1.0>
2nd line:	
Thickness of layer of each column in m (thickness must be > 0)	<100>
3rd line:	
Water depth of layer at time of deposition for each column in m	<50>
4th line:	
Composition of layer for each column, where 0 = sand and 1= shale	<1>

Then the velocity magnitude |v| and its direction, α, can be determined:

$$|v_{i,j}| = \sqrt{v_{xi,j}^2 + v_{zi,j}^2} \tag{6-71}$$

$$\tan\alpha = \frac{v_x}{v_z} \tag{6-72}$$

Data that the user must supply as input for the program consist of the grid specifications, including the grid size and grid spacing, properties such as fluid density and viscosity, initial basement topography, and specifications for the sedimentary layers, including their initial thicknesses and composition (Table 6-3). Output (Table 6-4) consists of a set of properties over the grid for each time step, including elevations, thicknesses, porosities, permeabilities, fluid pressures, and flow directions.

Table 6-4 Example program output from Program 24, Compaction and Fluid Flow Program. Program writes out following variables for evolving grid that represents vertical section through basin for each timestep:

Topographic elevations of each grid cell in m
Porosity
Vertical intrinsic permeability in millidarcies (md)
Lithostatic pressure or overburden load in megapascals (MPa)
Fluid pressure in MPa
Flow velocities in mm/year
Flow directions in degrees counterclockwise from north

Two simplified hypothetical simulation experiments are presented to demonstrate the effects of initial geometry, sedimentation rates, and sediment type on the evolution of pore fluid pressures, flow directions, and velocities in basins. Although synthetic, the experiments treat two common types of basins, where compaction and dewatering are important scientifically and economically (Tissot & Welte 1982). The first involves a "failed" rift (Experiment 6-1), and the second involves a delta building out over a continental margin (Experiment 6-2).

These experiments might be regarded as extremely simplified representations of basins such as the North Sea and the Gulf of Mexico adjacent to the Mississippi delta. The cross sections in the two experiments involve only ten columns, so that the input files and computing times are short. There is no lateral variation in sediment composition in the failed rift experiment (Experiment 6-1), and only limited lateral variation in the delta experiment (Experiment 6-2). Furthermore, there is no active structural deformation such as block faulting or growth faulting, which are sometimes important in actual basins. Nevertheless, the experiments show that sediment composition and rates of deposition may have significant effect on pore-fluid overpressures and motions in basins.

Table 6-5
Input file for Experiment 6-1.

```
10 9 10000
1025 2650 1.00
  0   0   0 -50 -100 -100 -50   0   0   0
1
  1   1   1  50  100  100  50   1   1   1
  0   0   0   0    0    0   0   0   0   0
  0   0   0   0    0    0   0   0   0   0
1
  5  10  20  30   40   40  30  20  10   5
  0   0   0   0    0    0   0   0   0   0
  0   0   0   0    0    0   0   0   0   0
1
 10  20  50 100  100  100 100  50  20  10
100 100 100 100  100  100 100 100 100 100
  1   1   1   1    1    1   1   1   1   1
2
 10  20  50 100  100  100 100  50  20  10
100 100 100 100  100  100 100 100 100 100
  1   1   1   1    1    1   1   1   1   1
3
 10  20  50 100  100  100 100  50  20  10
100 100 100 100  100  100 100 100 100 100
  1   1   1   1    1    1   1   1   1   1
5
 10  20  50 100  100  100 100  50  20  10
100 100 100 100  100  100 100 100 100 100
  1   1   1   1    1    1   1   1   1   1
8
 10  20  50 100  100  100 100  50  20  10
100 100 100 100  100  100 100 100 100 100
  1   1   1   1    1    1   1   1   1   1
10
 10  20  50 100  100  100 100  50  20  10
  0   0   0   0    0    0   0   0   0   0
  0   0   0   0    0    0   0   0   0   0
15
 10  20  50 100  100  100 100  50  20  10
  0   0   0   0    0    0   0   0   0   0
  0   0   0   0    0    0   0   0   0   0
```

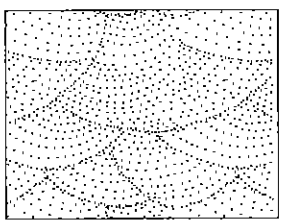

Experiment 6-1: Hypothetical Failed Rift

Experiment 6-1 involves the hypothetical failed rift. Its input (Table 6-5) reflects three distinct developmental phases, namely (1) an initial rift phase in which relatively permeable terrestrial sediments were deposited (0 to 2 million years), (2) a main rift phase during which there was rapid subsidence coupled with deposition of thick sequences of shale (3 to 5 million years), and (3) an abandoned rift phase involving moderate sedimentation rates in which mixtures of sandstones and shales were deposited (6 to 31 million years).

With regard to pore-fluid expulsion and development of overpressures, the fluid pressures at the outset are initially hydrostatic, but rapidly increase in shales during deposition (Color Plate 6-1), with fluid pressures markedly in excess of hydrostatic (Figure 6-3). Overpressures are accompanied by undercompacted sands in the lower part of the sequence (Figure 6-4). With the passage of time, however, there is gradual release of overpressures as deposition rates decline as the rift system is progressively abandoned (Color Plate 6-2).

Figure 6-3
Experiment 6-1 (failed-rift experiment): Plot of pressure in megapascals versus depth in meters for center column of grid section representing basin. Composition of sediment in column is shown schematically on right side of plot. Plot pertains to end of experiment, after 46 million years have elapsed. Lithostatic pressures due to sediment load are shown with solid diamonds, hydrostatic or normal fluid pressures are shown with open squares, and fluid pressures obtained in experiment are shown with solid squares. Note that while hydrostatic gradient remains constant, lithostatic pressure varies as result of high compactibility of shales, and fluid pressures obtained in experiment are markedly higher than hydrostatic within thick shale unit, as well as in basal sands.

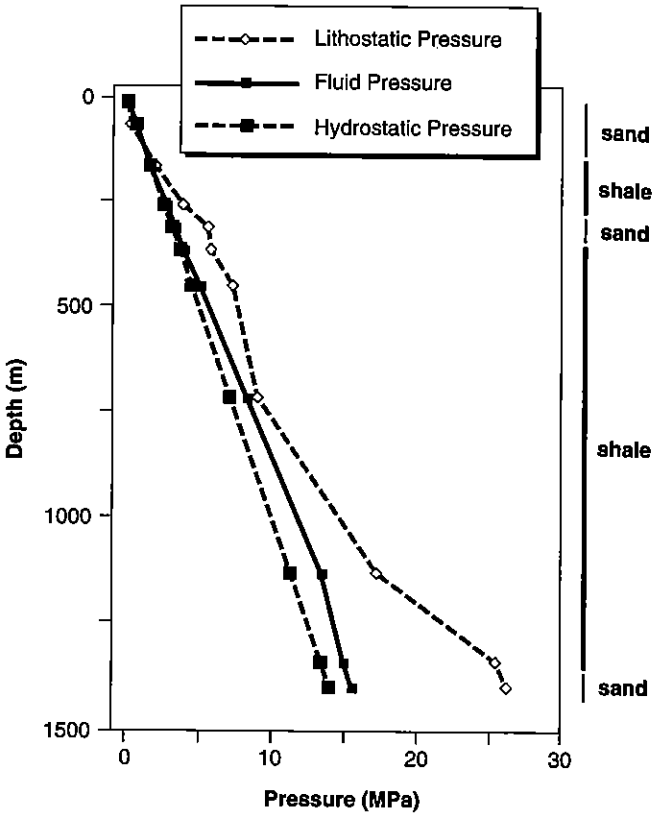

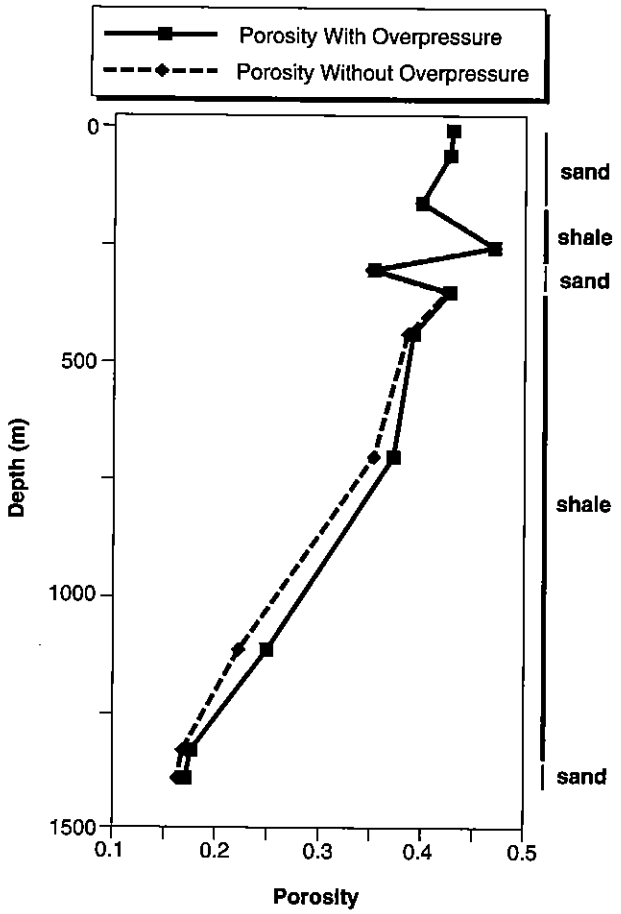

Figure 6-4
Experiment 6-1 (failed-rift experiment): Plot of porosity versus depth for center column of grid section representing basin. Composition of sediment in column is shown schematically on right side of plot. Plot pertains to end of experiment, after 46 million years have elapsed. Porosities under hydrostatic conditions (without overpressures) are denoted with solid diamonds, whereas porosities under conditions in experiment in which overpressures occur, are shown with open squares. Note that undercompaction is greatest within thick shale interval, but sand at base of column is also undercompacted.

Table 6-6 Input file for Experiment 6-2.

```
10 5 10000
1025 2650 1.00
  0   0 -10 -20 -50 -80 -90 -100 -100 -100
1
 20  20  30  50  80 100  50  30  20  10
  0   0 -10 -20 -50 -80 -90 -100 -100 -100
  0   0   0   1   1   1   1   1   1   1
1
 20  20  20  50 100 300 500 300 200 100
  0   0 -10 -20 -50 -80 -90 -100 -100 -100
  0   0   0   1   1   1   1   1   1   1
1
 20  20  20  50 100 300 500 500 300 100
  0   0 -10 -20 -50 -80 -90 -100 -100 -100
  0   0   0   0   1   1   1   1   1   1
1
 20  20  20  50 100 200 300 500 500 300
  0   0 -10 -20 -50 -80 -90 -100 -100 -100
  0   0   0   0   1   1   1   1   1   1
1
 20  20  20  20  50 100 300 500 500 500
  0   0 -10 -20 -50 -80 -90 -100 -100 -100
  0   0   0   0   0
              1   1   1   1   1
```

Experiment 6-2: Hypothetical Rapidly Growing Delta

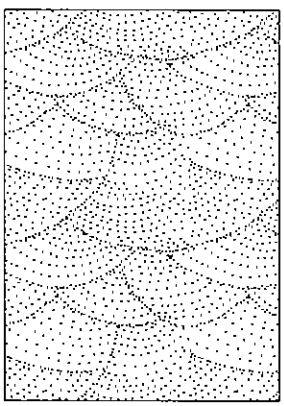

Experiment 6-2 involves prograding wedges that create a delta complex containing thickened prodelta muds and shales that form partly in response to increased subsidence toward their downdip components (Table 6-6). With respect to pore-fluid expulsion and the evolution of changes in fluid pressures, there is steady increase in the degree of overpressure in the shales (Color Plate 6-3). We note, also, that there is topographically driven flow in the recharge area.

We can alter the system by incorporating a static vertical "fault." This is achieved by simply changing a grid column within the shales so that it is represented by sand (which is highly permeable) instead of shale, thereby creating a conduit for flow. While somewhat unrealistic because a very wide zone is created, the effect would be similar even if narrower and more realistic. Flow is focused within the column of sand and overpressures are greatly reduced (Color Plate 6-4).

SUMMARY

Compaction and dewatering of sediment and other porous materials can be treated as integral processes. Darcy's law provides the starting point in our consideration of flow through porous materials. By linking Darcy's law with the Bernoulli equation, which represents the forces acting on a volume of fluid in terms of hydraulic heads, Darcy's law yields a momentum equation which successively can be linked with compaction. If compaction due to the overlying load is to occur, any change in effective stress imposed by the overlying load must be compensated by change in pore-fluid pressure. This relationship permits changes in porosity to be defined

as a function of changes in pore-fluid pressure, leading to the classical equation of consolidation.

The motions of both a compacting solid and the pore fluid being expelled can be represented in a spatial coordinate system, which in our application is simplified as a two-dimensional grid that forms a vertical section through an evolving sedimentary basin. By obtaining a general diffusion equation for the pore-fluid motions in the basin, we can prepare a series of numerical solutions for it after it has been transformed into finite form. The numerical solutions are provided at a series of timesteps that represent successive increments of time in the evolving basin. We supply initial and boundary conditions for the numerical solutions, and provide functions that relate porosity to effective stress, and permeability to porosity.

The numerical solutions are graphically displayed, providing us with a series of snapshots of the evolving basin as compaction takes place in response to load, and pore fluid moves through the sequence of beds in the expulsion process. Contours show changes in transient overpressures as the overlying load is partially transmitted to the moving pore fluid.